bioRxiv preprint doi: https://doi.org/10.1101/614412; this version posted April 21, 2019. The copyright holder for this preprint (which was not certified by peer review) is the author/funder. All rights reserved. No reuse allowed without permission.

A Genetically Encoded Fluorescent Sensor Enables Real-time Detection of the Intracellular GTP:GDP Ratio

*Jiayuan Zhang[a]+, Yuxin Song[a]+, Shuzhang Liu[b], Weibo Wang[c], Meiqi Zhang[a], Guangfu Yang[c], Peng Zou[b], and Jing Wang[a]**

Abstract: *The interconversion of guanosine triphosphate (GTP) and guanosine diphosphate (GDP) is integral to a wide variety of biological cellular activities. However, analytical methods which directly detect the ratio of intracellular GTP and GDP concentrations have not been available. Herein, we report GNEPS, a genetically encoded fluorescent sensor that enables real-time monitoring of the GTP:GDP ratio, which is a fusion protein comprising a eukaryotic G-protein and a circularly permuted yellow fluorescent protein. GNEPS has distinct fluorescence spectra between its GTP-bound and GDP-bound states. Its apparent fluorescence signal therefore depends upon the competitive binding of GTP and GDP. Live cell imaging experiments demonstrated that GNEPS can be used to monitor spatiotemporal changes in the intracellular GTP:GDP ratio in various cell types and organelles in response to metabolic perturbations. We anticipate that GNEPS will become a valuable tool for understanding the metabolic and regulatory contributions of guanosine nucleotides.*

WITHDRAWN
See manuscript DOU for details.

Guanosine nucleotides are important components of cellular energy metabolism. GTP and GDP are essential to a huge diversity of physiological processes, and they function as co-factors in myriad enzymatic reactions. Indeed, core metabolic processes including protein synthesis and gluconeogenesis are driven by energy released from the hydrolysis of GTP into GDP.[1] At the regulatory level, GTP and GDP are known to control the functions of G-proteins, which oscillate between a GTP-bound "on" state and a GDP-bound "off" state in a reversible manner;[2] the transition between these two states regulates cellular activities like signal transduction[3] and mitosis.[4] Thus, knowledge of the relative concentrations of intracellular GTP to GDP represents a highly informative indicator of both cellular energy status and G-protein activation. Highlighting the impact of these guanosine nucleotides in biology generally, studies in many life science research areas require monitoring of GTP and GDP levels, and to date these measurements have typically employed HPLC-based methods.[5,6] However, given that such methods require cell lysis during sample preparation, they inevitably result in the loss of biologically relevant spatial and temporal information. Several fluorescent sensors have also been developed to detect GTP,[7-9] but to our knowledge, there are currently no reported fluorescent sensors for directly monitoring the GTP:GDP ratio in live cells.

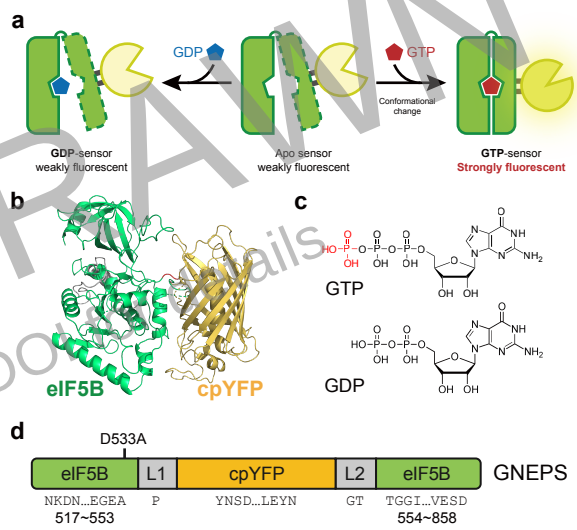

Figure 1. Design and construction of GNEPS. a) Proposed mechanism of a fluorescent sensor for the GTP:GDP ratio. b) Simulated structure of GNEPS. eIF5B and cpYFP are shown in green and yellow, respectively. Peptide linkers are shown in red. c) Chemical structures of GTP and GDP. d) Schematic representation of GNEPS.

Herein, we present the development of a genetically encoded fluorescent sensor that is capable of visualizing the GTP:GDP ratio in live cells. Our sensor harnesses a known ligand-induced conformational change in the *Chaetomium thermophilum* eIF5B protein (Ct-eIF5B), a eukaryotic translational initiation factor capable of binding both GTP and GDP. Crystal structures of Ct-eIF5B[10,11] have revealed that binding of GTP but not GDP triggers dramatic conformational changes in two conserved regions termed switch 1 and switch 2 of eIF5B domain I (Figure S1a). In addition to this binding-induced conformational change, eIF5B is also an attractive candidate scaffold for sensor design because of its fast GTP-GDP exchange rate and because its exchange capacity does not require a dedicated guanosine nucleotide exchange factor.[12]

To transform the ligand-induced conformational change of eIF5B into a measurable fluorescence signal, we designed a series of fusion proteins by combining eIF5B with a circularly permuted yellow fluorescent protein (cpYFP) which was originally reported as part of a hydrogen peroxide sensor (HyPer)[13] (Figure 1a and 1b).

As the fluorescence of cpYFP was highly sensitive to protein conformation, we computationally explored differences in C α dihedral angles between the apo and GTP-bound states of eIF5B, as this difference should be indicative of the magnitude of local conformational changes around certain amino acid

[a] J. Zhang,[+] Y. Song,[+] M. Zhang, Prof. J. Wang
State Key Laboratory of Natural and Biomimetic Drugs
Department of Chemical Biology, School of Pharmaceutical Sciences
Peking University, Beijing 100191, China
E-mail: wangjingsioc@pku.edu.cn
[b] S. Liu, Prof. P. Zou
College of Chemistry and Molecular Engineering
Synthetic and Functional Biomolecules Center
Peking University, Beijing 100871, China
[c] W. Wang, Prof. G. Yang
Key Laboratory of Pesticide and Chemical Biology
College of Chemistry, Ministry of Education
Central China Normal University, Wuhan 430079, China
[+] These authors contributed equally to this work

Supporting information for this article is given via a link at the end of the document.

bioRxiv preprint doi: https://doi.org/10.1101/614412; this version posted April 21, 2019. The copyright holder for this preprint (which was not certified by peer review) is the author/funder. All rights reserved. No reuse allowed without permission.

residues.[14] This analysis identified switch 1 and switch 2, as well as the hinge between domain I and domain II of eIF5B as hotspots for large structural changes (Figure S1b). Accordingly, We selected 16 positions within these regions for cpYFP insertion and generated the corresponding recombinant fusion proteins. Among them, the fusion protein with cpYFP inserted after the A553 residue of eIF5B domain I displayed the highest fluorescence change between its GTP-bound and GDP-bound states (i.e., its dynamic range), and was thus selected as the scaffold for subsequent optimization (Figure S1c).

Next, we engineered this eIF5B-cpYFP fusion protein in three steps to improve its performance as a fluorescent sensor. First, we substituted cpYFP from HyPer with another two cpYFP variants,[15,16] but neither of them offered a higher dynamic range than the original cpYFP (Figure S2). Second, several point mutations were incorporated into the nucleotide binding pocket of eIF5B (Figure S3a). After screening, we preserved the D533A mutation, as it lead to a 38% increase in the dynamic range (Figure S3b). Importantly, this mutation has been demonstrated to abolished eIF5B's intrinsic GTPase activity,[11] so its incorporation prevents any catalysis-mediated depletion of the cellular GTP reservoir. Finally, we randomly altered the linker residues spanning both ends of cpYFP with degenerate primers[17] (Figure S3c), and selected a linker pair consisting of an N-terminal Pro linker and a C-terminal Gly-Thr linker for its highest dynamic range (Figure S3d). The resulting fusion protein was named GNEPS (Guanosine Nucleotide Energy Potential Sensor, Figure 1d and Appendix 1).

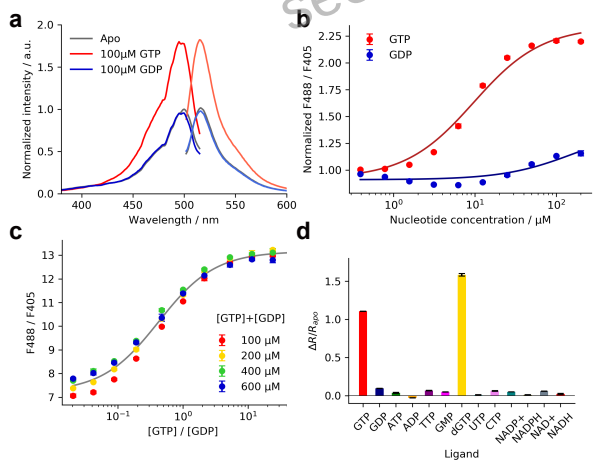

Figure 2. Characterization of purified GNEPS. a) Fluorescence excitation and emission spectra of purified GNEPS in the apo state and after addition of 100μM GTP or 100μM GDP. Fluorescence intensity was normalized to the peak intensity in the apo state. b) Normalized fluorescence intensity ratio of GNEPS excited at 488nm and 405nm (F488/F405) plotted against concentrations of GTP or GDP. Emission was measured at 517nm (n = 4). c) Fluorescence response of GNEPS to the GTP:GDP ratio at the indicated total guanosine nucleotide concentrations (n = 3). The function between F488/F405 signal and [GTP]/[GDP] was modeled by a competitive binding model (gray curve). d) Fluorescence response of GNEPS to the addition various nucleotides at a concentration of 100μM (n = 3). All error bars denote the SD.

To further characterize its fluorescence response to GTP and GDP, we purified GNEPS with size exclusion chromatography (Figure S4) and found that it had an excitation peak at 499 nm and an emission peak at 517 nm. The addition of GTP altered the excitation spectra, leading to an enhancement of the 499nm peak and a slight decrease around 420 nm, resulting in a one-fold change in the ratio of emission intensities at 488 nm and 405 nm excitation (F488/F405). In contrast, the addition of GDP only induced a marginal change (Figure 2a and 2b). This finding is consistent with previous reports that only GTP binding could trigger a substantial conformational change in eIF5B domain I.

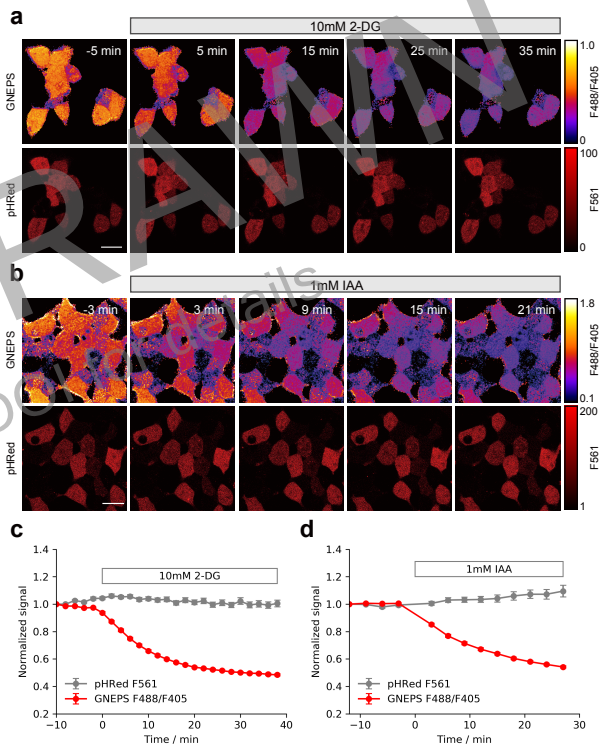

Figure 3. Imaging GTP:GDP dynamics in HEK293T cells. a) Representative images of HEK293T cells co-expressing GNEPS and pHRed before and after treatment with 10mM 2-Deoxy-D-glucose (2-DG). The GNEPS signal is presented as pixel-by-pixel ratio between the 488nm excitation image and the 488nm excitation image. Scale bar: 20μm. b) Representative images of HEK293T cells co-expressing GNEPS and pHRed before and after treatment with 1mM iodoacetic acid (IAA). Scale bar: 20μm. c) Kinetics of GNEPS and pHRed fluorescence response in HEK293T cells as in (a) (n = 33 cells). d) Kinetics of GNEPS and pHRed fluorescence responses in HEK293T cells as in (c) (n = 27 cells). All error bars denote the SEM.

Since GTP- and GDP-bound GNEPS displayed divergent fluorescence spectra, the observed fluorescence signals should reflect the relative concentration of the two nucleotides: the GTP:GDP ratio.[15,18] To confirm this, we measured the F488/F405 signal of purified GNEPS after the addition of GTP-GDP mixtures of different total (100μM to 600μM) and relative (49:1 to 1:49) concentrations. As predicted, the fluorescent response of GNEPS was a function of GTP:GDP ratio alone, regardless of their total concentrations (Figure 2c). The signal was well approximated by a competitive binding model ($K_{d,GTP}/K_{d,GDP}$ = 0.41). In addition, we confirmed that the response of GNEPS to the GTP:GDP ratio was not significantly affected by the presence of ATP, ADP, NADH,

WITHDRAWN
see manuscript Decision Details

bioRxiv preprint doi: https://doi.org/10.1101/614412; this version posted April 21, 2019. The copyright holder for this preprint (which was not certified by peer review) is the author/funder. All rights reserved. No reuse allowed without permission.

WITHDRAWN
see nonubmit DOI for details

NAD^+, NADPH, or $NADP^+$ (Figure S5a and 5b), nor by changes in their relative concentration ratios (Figure S5c-e). These results establish that GNEPS is a robust sensor that specifically reports the GTP:GDP ratio.

Apart from GTP and GDP, the addition of other biologically relevant nucleotides to solutions containing purified GNEPS did not trigger any obvious signal changes, with the exception of dGTP (Figure 2d). Considering that the intracellular concentrations of GTP and GDP usually exceed the dGTP concentration by over 100-fold,[19] the effect of dGTP binding on the GNEPS response should be minimal under physiological conditions; this was confirmed by recording the response of GNEPS to GTP:GDP in the presence of various concentrations of dGTP (Figure S5f).

Similar to most cpFP-based biosensors, the fluorescence of GNEPS is sensitive to variations in pH. Our data indicated that GNEPS was capable of sensing the GTP:GDP ratio in the pH range of 7.0~7.8 (Figure S6a). Normalization of the GNEPS response at different pH to the range of 0~1 revealed that the relative affinity for GTP and GDP was not affected by pH (Figure S6b). GNEPS was also robust to temperature changes within the range of 25–37℃ (Figure S6c).

Cellular GTP and GDP exist predominately in their Mg^{2+}-bound forms.[20] We therefore investigated the dependence of Mg^{2+} on the GNEPS response. GNEPS could not differentiate GTP and GDP in the absence of Mg^{2+}, but the response recovered to a stable level after the addition of submillimolar Mg^{2+}(Figure S6d), indicating that GNEPS is functional under physiological concentrations of Mg^{2+} (0.5~5mM).[21]

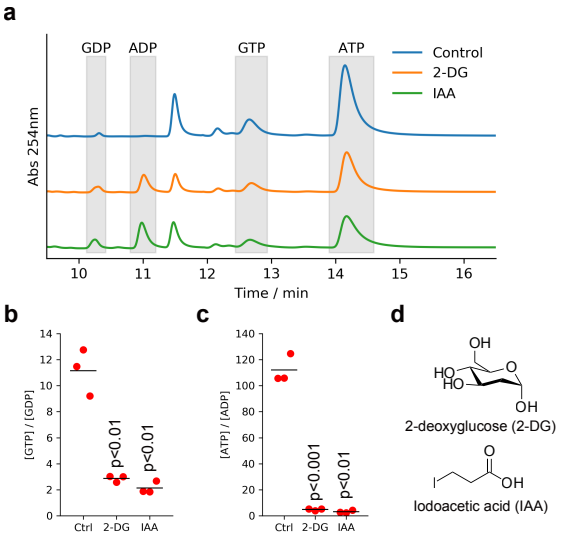

Figure 4. HPLC analysis of intracellular GTP:GDP ratio. a) Representative HPLC chromatogram of nucleotide extracts from HEK293T cells with or without treatment by 2-DG (30min) or IAA (15min). b, c) Calculated intracellular GTP:GDP ratios (b) and ATP:ADP ratios (c) in HEK293T cells as in (a) (n = 3 biological replicates). *P* values were calculated with the two-tailed Student's *t*-test. d) Chemical structures of 2-DG and IAA.

Having characterized the properties and performance of purified GNEPS, we next evaluated the utility of GNEPS for sensing intracellular GTP:GDP ratio dynamics. We initially expressed the sensor in human embryonic kidney (HEK293T) cells via transient transfection. In these experiments, the pHRed[22] sensor (Figure S7) was co-transfected as a control to monitor pH fluctuations. GNEPS and pHRed fluorescence were recorded simultaneously in three channels: 405nm/488nm excitation for GNEPS and 561nm excitation for pHRed (Figure S8).

As the intracellular GTP:GDP ratio has been reported to correlate tightly with glucose catabolism and the ATP:ADP ratio,[23,24] we first treated transfected HEK293T cells with 2-Deoxy-D-glucose (2-DG), a non-metabolizable derivative of glucose that inhibits glycolysis. As expected, the F488/F405 readout of GNEPS decreased gradually to around 50% of its initial value by 40 min after 2-DG treatment, while the pHRed signal remained practically constant, indicating a stable intracellular pH (Figure 3a and 3c). Iodoacetic acid (IAA), another glycolysis inhibitor, had a similar but more rapid effect on HEK293T cells (Figure 3b and 3d).

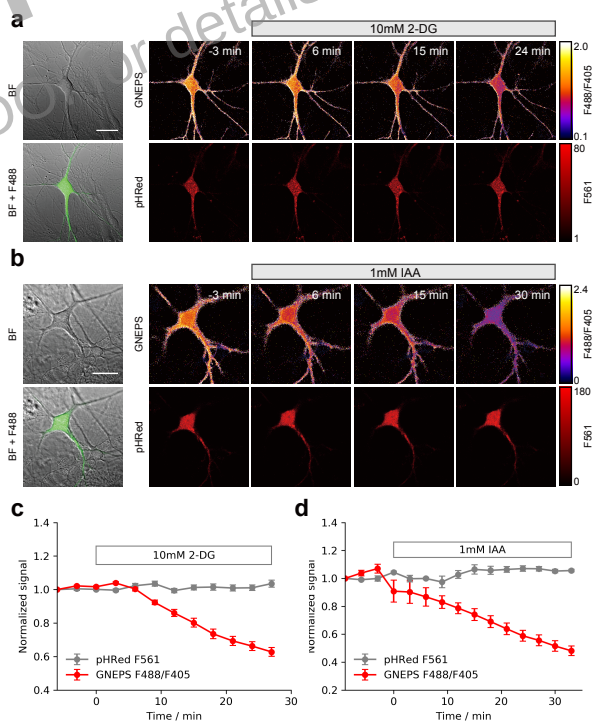

Figure 5. Applying GNEPS in cultured primary neurons. a) Representative images of rat primary neuron cells co-expressing GNEPS and pHRed before and after treatment with 10mM 2-DG. Scale bar: 30μm. b) Representative images of primary neuron cells co-expressing GNEPS and pHRed before and after treatment with 1mM IAA. Scale bar: 30μm. c) Kinetics of GNEPS and pHRed fluorescence responses in HEK293T cells as in (a) (n = 16 cells). d) Kinetics of GNEPS and pHRed fluorescence responses in HEK293T cells as in (c) (n = 5 cells). All error bars denote the SEM.

We then used a standard HPLC-based method to measure the effects of 2-DG and IAA on intracellular nucleotide pools. After 2-DG/IAA treatment, we observed decreases in GTP and ATP peaks that were accompanied by increases in the GDP and ADP peaks (Figure 4a). Interpolating the respective standard curves

bioRxiv preprint doi: https://doi.org/10.1101/614412; this version posted April 21, 2019. The copyright holder for this preprint (which was not certified by peer review) is the author/funder. All rights reserved. No reuse allowed without permission.

for the GTP:GDP and ATP:ADP ratios (Figure S9) revealed dramatic decreases for both the GTP:GDP and ATP:ADP ratios upon 2-DG/IAA treatment in HEK293T cells (Figure 4b and 4c). Additionally, no significant response was observed when we added 2-DG or IAA to purified GNEPS (Figure S10). These results collectively demonstrate that GNEPS can sense and report cellular dynamic changes in guanosine nucleotide metabolism in real time.

The activities of small G-proteins have essential functions in neuronal plasticity and memory formation,[25] and we next explored the use of our sensor in primary neuron cultures isolated from rat hippocampi. We observed a uniform distribution of GNEPS signal across the cell bodies, axons, and dendrites of isolated rat hippocampus neurons, revealing that the GTP:GDP ratio is apparently constant in these diverse structures. After treatment with 2-DG and IAA, we observed inhibition effects that were very similar to those observed in HEK293T cells (Figure 5).

The ability to be targeted into particular organelles is a major advantage of genetically encoded sensors over small-molecule probes. To demonstrate this important feature, we expressed constructs for GNEPS and pHRed that included nuclear localization sequence (NLS) peptides in HEK293T cells and in neurons. Upon IAA treatment, we observed a nucleus-specific decrease in the GNEPS signal in both cell types (Figure S11), in agreement with our expectation that the guanosine nucleotide pools in the cytosol and in nuclei are kept in equilibrium by passive diffusion through nuclear pores.[26] These results highlight the adaptability of GNEPS for use in different cell types and organelles.

In conclusion, we have successfully developed GNEPS, a genetically-encoded fluorescent sensor for GTP:GDP ratio that offers excellent selectivity and robustness. To our knowledge, GNEPS is the first biosensor for monitoring fluctuations in GTP:GDP ratio in live cells. Collectively, our results demonstrate that GNEPS, which can be conveniently incorporated into cells and sub-cellular compartments, substantially advances the ability of life scientists to visualize the spatiotemporal dynamics of guanosine nucleotide metabolism. Further application of GNEPS may facilitate high-throughput screening of specific activators and inhibitors that affect the GTP-GDP interconversion, as well as elucidation of the regulation networks of G-protein activation *in vitro* and *in vivo*.

Acknowledgements

This work supported by the National Basic Research Foundation of China (No. 2017YFA0505202 to J. W.), the National Natural Science Foundation of China (91853107 to J. W.). J. W. also thanks the Youth Thousand-Talents Program of China for support.

Conflict of interest

The authors declare no conflict of interest.

Keywords: biosensor • cell imaging • fluorescent probes • GTP:GDP ratio • protein engineering

[1] J. M. Berg, J. L. Tymoczko, L. Stryer, *Biochemistry*, W.H. Freeman, Basingstoke, **2012**, p. 481, 905.
[2] R. Gasper, S. Meyer, K. Gotthardt, M. Sirajuddin, A. Wittinghofer, *Nat. Rev. Mol. Cell Biol.* **2009**, *10*, 423–429.
[3] W. M. Oldham, H. E. Hamm, *Nat. Rev. Mol. Cell Biol.* **2008**, *9*, 60-71.
[4] P. R. Clarke, C. Zhang, *Nat. Rev. Mol. Cell Biol.* **2008**, *9*, 464-477.
[5] M. H. Buckstein, J. He, H. Rubin, *J. Bacteriol.* **2008**, *190*, 718-726.
[6] P. Chen, Z. Liu, S. Liu, Z. Xie, J. Aimiuwu, J. Pang, R. Klisovic, W. Blum, M. R. Grever, G. Marcucci, et al., *Pharm. Res.***2009**, *26*, 1504-1515.
[7] N. Ahmed, B. Shirinfar, I. S. Youn, A. Bist, V. Suresh, K. S. Kim, *Chem. Commun. (Cambridge, U. K.)* **2012**, *48*, 2662.
[8] S. Wang, Y.-T. Chang, *J. Am. Chem. Soc.* **2006**, *128*, 10380-10381.
[9] A. Bianchi-Smiraglia, M. S. Rana, C. E. Foley, L. M. Paul, B. C. Lipchick, S. Moparthy, K. Moparthy, E. E. Fink, A. Bagati, E. Hurley, et al., *Nat. Methods* **2017**, *14*, 1003-1009.
[10] B. Kuhle, R. Ficner, *EMBO J.* **2014**, *33*, 1177-1191.
[11] B. Kuhle, R. Ficner, *EMBO J.* **2014**, *33*, 2547-2563.
[12] V. P. Pisareva, C. U. T. Hellen, T. V. Pestova, *Biochemistry* **2007**, *46*, 2622-2629.
[13] V. V. Belousov, A. F. Fradkov, K. A. Lukyanov, D. B. Staroverov, K. S. Shakhbazov, A. V. Terskikh, S. Lukyanov, *Nat. methods* **2006**, *3*, 281-286.
[14] J. S. Marvin, E. R. Schreiter, I. M. Echevarría, L. L. Looger, *Proteins: Struct., Funct., Bioinf.* **2011**, *79*, 3025-3036.
[15] J. Berg, Y. P. Hung, G. Yellen, *Nat. methods* **2009**, *6*, 161-166.
[16] T. Nagai, A. Sawano, E. S. Park, A. Miyawaki, *Proc. Natl. Acad. Sci. U. S. A.* **2001**, *98*, 3197-3202.
[17] D. C. Nadler, S.-A. Morgan, A. Flamholz, K. E. Kortright, D. F. Savage, *Nat. Commun.* **2016**, *7*, 12266.
[18] Y. Zhao, Q. Hu, F. Cheng, N. Su, A. Wang, Y. Zou, H. Hu, X. Chen, H.-M. Zhou, X. Huang, et al., *Cell Metab.* **2015**, *21*, 777-789.
[19] T. W. Traut, *Mol. Cell. Biochem.* **1994**, *140*, 1-22.
[20] T. Simonson, P. Satpati, *J. Comput. Chem.* **2013**, *34*, 836-846.
[21] A. M. P. Romani, *Arch. Biochem. Biophys.* **2011**, *512*, 1-23.
[22] M. Tantama, Y. P. Hung, G. Yellen, *J. Am. Chem. Soc.* **2011**, *133*, 10034-10037.
[23] E. D. Schwoebel, T. H. Ho, M. S. Moore, *J. Cell Biol.* **2002**, *157*, 963-974.
[24] P. Detimary, G. Van den Berghe, J.-C. Henquin, *J. Biol. Chem.* **1996**, *271*, 20559-20565.
[25] X. Ye, T. J. Carew, *Neuron* **2010**, *68*, 340-361.
[26] B. L. Timney, B. Raveh, R. Mironska, J. M. Trivedi, S. J. Kim, D. Russel, S. R. Wente, A. Sali, M. P. Rout, *J. Cell Biol.***2016**, *215*, 57-76.

WITHDRAWN
see manuscript DOI for details